



Klotho overexpression improves amyloid- β clearance and cognition in the APP/PS1 mouse model of Alzheimer's disease

Yue Zhao | Chen-Ye Zeng | Xiao-Hong Li | Ting-Ting Yang | Xi Kuang | Jun-Rong Du

Department of Pharmacology, Key Laboratory of Drug-Targeting and Drug Delivery System of the Education Ministry and Sichuan Province, Sichuan Engineering Laboratory for Plant-Sourced Drug and Sichuan Research Center for Drug Precision Industrial Technology, West China School of Pharmacy, Sichuan University, Chengdu, China

Correspondence

Jun-Rong Du, Department of Pharmacology, Sichuan University, Chengdu 610041, China.
Email: dujr_1@163.com

Funding information

Fundamental Research Funds for the Central Universities; National Natural Science Foundation of China, Grant/Award Number: 81473219 and 81973307; 111 Project of the National Ministry of Education, Grant/Award Number: B18035

Abstract

Alzheimer's disease (AD) is the most prevalent type of dementia, characterized by the presence of amyloid- β (A β) plaques. We previously reported that Klotho lowered A β levels in the brain and protected against cognitive deficits in amyloid precursor protein/presenilin 1 (APP/PS1) mice. However, the underlying mechanism remains unclear. In this study, we induced intracerebral Klotho overexpression in 13-month-old APP/PS1 mice by injecting lentivirus that carried full-length mouse Klotho cDNA in the lateral ventricle of the brain. We examined the effects of Klotho overexpression on cognition, A β burden, A β -related neuropathology, microglia transformation, and A β transport systems in vivo. Additionally, we investigated the effects of Klotho on A β transport at the blood-cerebrospinal fluid barrier by knocking down Klotho in primary human choroid plexus epithelial cells (HCPEpiCs). The upregulation of Klotho levels in the brain and serum significantly ameliorated A β burden, neuronal and synaptic loss and cognitive deficits in aged APP/PS1 mice. Klotho treatment significantly inhibited NACHT, LRR, and PYD domain-containing protein 3 (NLRP3) and the subsequent transformation of microglia to the M2 type that may enhance microglia-mediated A β clearance. Meanwhile, Klotho overexpression also regulated A β transporter expression, which may promote A β transporter-mediated A β clearance. Moreover, the ability of HCPEpiCs to transport A β in vitro was also significantly impaired by Klotho knockdown. Given the neuroprotective effect of Klotho overexpression, the present findings suggest that Klotho should be further investigated as a potential therapeutic target for AD.

KEYWORDS

Alzheimer's disease, A β clearance, Klotho

Yue Zhao, Chen-Ye Zeng, Xiao-Hong Li are co-first authors.

This is an open access article under the terms of the Creative Commons Attribution License, which permits use, distribution and reproduction in any medium, provided the original work is properly cited.

© 2020 The Authors. *Aging Cell* published by Anatomical Society and John Wiley & Sons Ltd



1 | INTRODUCTION

Alzheimer's disease (AD) is a chronic age-related neurodegenerative disease that is mainly characterized by senile plaque deposition, intracellular neurofibrillary tangles, and progressive cognitive decline (Masters et al., 2015). As of 2018, more than 50 million cases of AD were diagnosed worldwide. Various hypotheses have been proposed to explain the etiology and pathogenesis of Alzheimer's disease. The amyloid- β ($A\beta$) cascade hypothesis is the mainstream hypothesis that has been used over the past two decades to explain the pathogenesis of AD (Hardy & Higgins, 1992). An imbalance of the production and clearance of $A\beta$ peptide is observed in the brains of AD patients, which subsequently form amyloid plaques and cause neuronal dysfunction (Selkoe & Hardy, 2016).

The deficiency of $A\beta$ clearance rather than $A\beta$ overproduction should be considered a major causal factor, which in turn may trigger neuroinflammation, progressive synaptic loss, and ultimately cognitive decline (Nalivaeva & Turner, 2019). Studies have shown that the activation of NACHT, LRR, and PYD domain-containing protein 3 (NLRP3) inflammasome by $A\beta$ mediates the transformation of microglia from the M2 type to M1 type, reducing the clearance of $A\beta$ (Frautschy et al., 1998; Heneka et al., 2013). Thus, a vicious feedback loop is formed between $A\beta$ and activation of the NLRP3 inflammasome, leading to progressive deterioration (Sheedy et al., 2013). Alterations of the expression or activity of efflux transporters (e.g., low-density lipoprotein receptor-related protein 1 [LRP1], P-glycoprotein [P-gp], and adenosine triphosphate [ATP]-binding cassette transporter A1 [ABCA1]) and the influx transporter receptor for advanced glycation end products (RAGE) were observed in AD patients and mouse models, resulting in impairments in the clearance of $A\beta$ (Chiu et al., 2015; Elali & Rivest, 2013). Inhibiting the NLRP3/caspase-1 axis and enhancing transporter-mediated $A\beta$ clearance may theoretically prevent the development of AD.

The anti-aging gene *Klotho* is highly expressed in the kidneys and choroid plexus, with lower expression in brain parenchyma (Kuro-o et al., 1997; Kurosu et al., 2005; Lim et al., 2015). *Klotho* has various physiological functions, such as anti-neuroinflammatory effects and the regulation of autophagy (Bian, Neyra, Zhan, & Hu, 2015; Xu & Sun, 2015). Previous studies showed that *Klotho* in the brain of AD patients and mouse models was significantly lower than in age-matched healthy groups (Dubal et al., 2015; Kuang et al., 2017; Massó

et al., 2015; Semba et al., 2014). More researches have provided indications that *Klotho* may alleviate an array of neurodegenerative diseases (Jamali-Raeufy et al., 2017; Dubal et al., 2015; Scazzone et al., 2019; Zeldich et al., 2019). These findings provide convincing evidence that *Klotho* may be a novel therapeutic target for the treatment of AD. In a previous study, we maintained intracerebral *Klotho* upregulation in 7-month-old amyloid precursor protein/presenilin 1 (APP/PS1) mice for up to 3 months, which significantly reduced $A\beta$ levels and attenuated cognitive dysfunction (Zeng et al., 2019). However, the effects of long-term *Klotho* upregulation on the late stage of AD and the underlying mechanism remain unclear.

Based on accumulating evidence of anti-AD effects of *Klotho*, we hypothesized that *Klotho* ameliorates $A\beta$ pathology and cognitive impairment by promoting the transformation of microglia from M1 type to M2 type and regulating $A\beta$ transporter function. In the present study, we maintained *Klotho* overexpression for 6 months in APP/PS1 mice and evaluated the role of the NLRP3 inflammasome in microglia transformation and $A\beta$ transporter expression at the blood-brain barrier (BBB) and blood-cerebrospinal fluid (CSF) barrier. We also knocked down *Klotho* in human primary choroid plexus epithelial cells (HCPEpiCs) and evaluated the effect of *Klotho* on $A\beta$ transport clearance across the blood-CSF barrier.

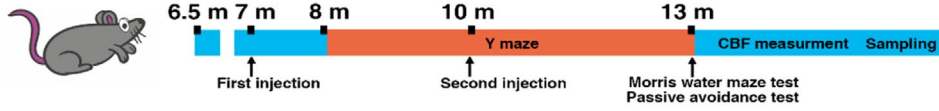
2 | RESULTS

2.1 | *Klotho* overexpression attenuated cognitive impairment in aged APP/PS1 mice

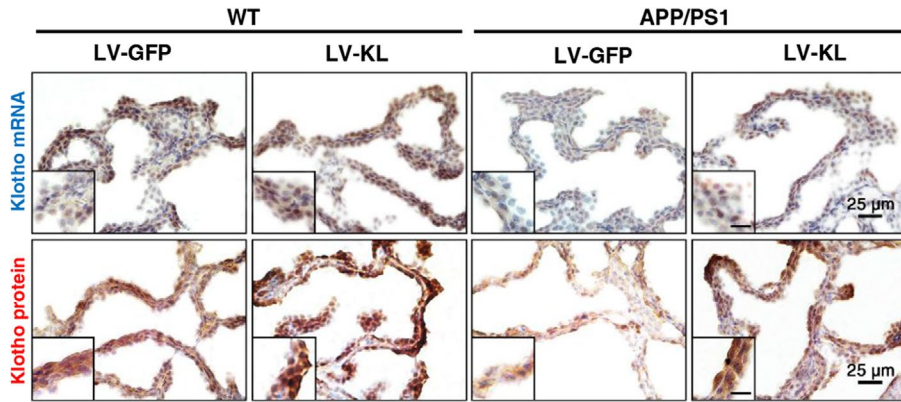
We first measured *Klotho* levels in the brain and serum when mice were 13 months old. Compared with the WT/LV-GFP group (WT, wide type; LV, lentivirus; GFP, green fluorescent protein), we observed a ~50% decrease in *Klotho* mRNA and protein levels in the choroid plexus and cerebrum in the APP/PS1/LV-GFP group. *Klotho* expression was significantly upregulated by LV-KL (KL, *Klotho*) in the cerebrum in WT mice and APP/PS1 mice (Figure 1b-e). Since cognitive function is closely related to hippocampus, we simultaneously measured the *Klotho* levels in hippocampus and found that similar to the trend of cerebrum, LV-KL also increased the mRNA and protein levels of *Klotho* in the hippocampus in WT mice and APP/PS1 mice (Figure 1b-e). Notably, LV-KL reversed the reduction of serum

FIGURE 1 *Klotho* overexpression attenuated cognitive impairment in aged APP/PS1 mice. (a) Temporal schematic diagram of the experimental procedures. (b) Representative images of *Klotho* mRNA and protein levels in the choroid plexus, detected by in situ hybridization and immunohistochemistry, respectively. The inset shows representative overall staining intensity. Scale bar = 10 μ m. (c) Quantitative image analysis of *Klotho* mRNA and protein levels based on the integrated optical density (IOD) of positive immunostaining (brown). (d) Analysis of *Klotho* mRNA levels in the hippocampus and cerebrum by quantitative real-time polymerase chain reaction (qRT-PCR). Relative *Klotho* mRNA levels were normalized to GAPDH and are expressed as fold changes relative to the WT/LV-GFP group. (e) *Klotho* levels in the hippocampus, cerebrum and serum were measured by enzyme-linked immunosorbent assay (ELISA). (f) Percentage of alternation in the Y-maze test. (g) Latency and number of errors in the passive avoidance test. (h) Escape latency, time in the target quadrant, number of platform crossings, and characteristic swimming trails in the Morris water maze. $n = 12$ /group, except $n = 6$ /group in (d, e). The data are expressed as mean \pm standard error of mean (SEM). The statistical analysis was performed using two-way analysis of variance (ANOVA) and mixed-design ANOVA (f, escape latencies in h) followed by the Bonferroni-Holm post hoc test. * $p < 0.05$, ** $p < 0.01$, vs. APP/PS1/LV-GFP group; ## $p < 0.01$, vs. WT/LV-GFP group

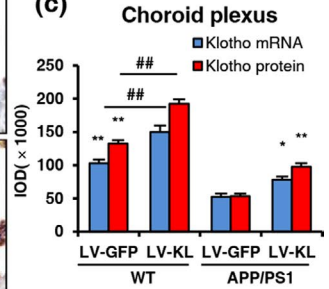
(a)



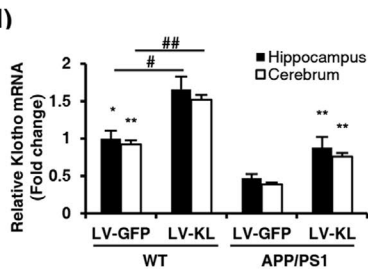
(b)



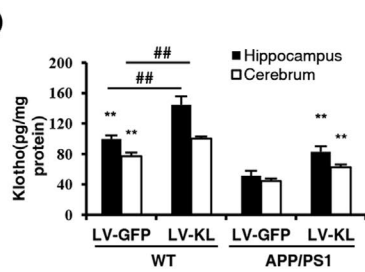
(c)



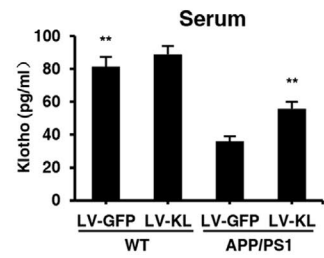
(d)



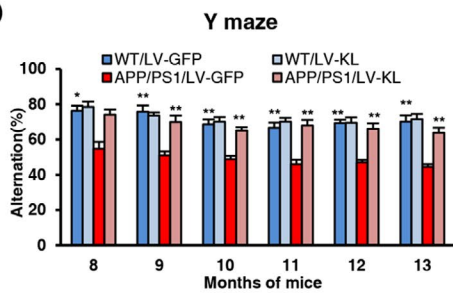
(e)



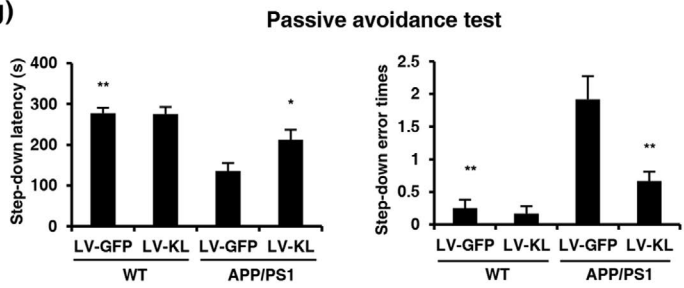
(f)



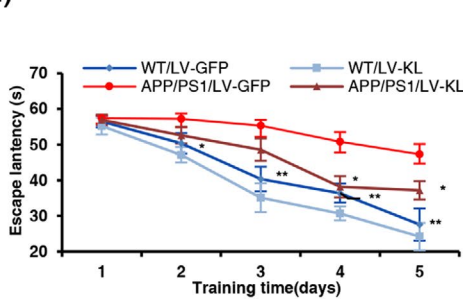
(f)



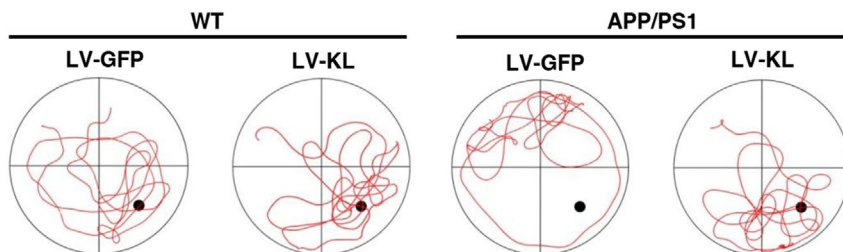
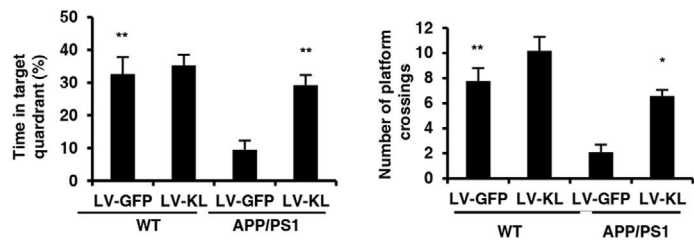
(g)



(h)



(i)





Klotho levels in APP/PS1 mice (Figure 1e). One possible way by which Klotho enters the blood is through the integrity loss of the BBB in APP/PS1 mice (Ahn et al., 2018; Takechi et al., 2010; Zhang et al., 2018). The current findings showed that LV-KL significantly upregulated Klotho expression in the brain in both WT and AD mice and upregulated serum Klotho level in AD mice.

Three neurobehavioral tests were performed to evaluate cognitive function. No significant differences were found between the WT/LV-GFP and WT/LV-KL groups. In the Y-maze (Figure 1f), the percentage of alternation in the APP/PS1/LV-GFP group was significantly lower than in the WT/LV-GFP group beginning at 8 months of age, which was significantly reversed by LV-KL. In the passive avoidance test (Figure 1g), the step-down latency significantly decreased, and the step-down error times significantly increased in the APP/PS1/LV-GFP group compared with the WT/LV-GFP group, and these changes were significantly reversed by LV-KL. In the Morris water maze (Figure 1h), the escape latency was significantly longer in the APP/PS1/LV-GFP group than in the WT/LV-GFP group, whereas the percent time in the target quadrant and number of platform crossings significantly decreased in the APP/PS1/LV-GFP group compared with the WT/LV-GFP group. Notably, LV-KL significantly improved these behavioral impairments in APP/PS1 mice. The current findings showed that Klotho overexpression ameliorated cognitive deficits in AD mice.

2.2 | Klotho overexpression decreased A β burden in aged APP/PS1 mice

The accumulation of A β results in AD lesions in APP/PS1 mice. We examined brain, serum, and cerebrovascular levels of A β in mice. No amyloid plaques were observed in WT mice. LV-KL treatment resulted in a 40%–50% reduction of A β plaques in the hippocampus and cortex in APP/PS1 mice (Figure 2a,b). LV-KL significantly decreased the levels of soluble and insoluble A β_{1-40} and A β_{1-42} in the brain in the APP/PS1/LV-GFP group (Figure 2c). Serum levels of soluble A β_{1-40} and A β_{1-42} in the APP/PS1/LV-GFP group were also reduced by LV-KL (Figure 2d).

Failure of the brain to clear excessive A β may lead to vascular A β deposition and subsequently cause cerebral amyloid angiopathy (CAA) (Greenberg et al., 2020). Double-staining for A β (red) and laminin (green) elucidated the effects of Klotho on CAA. No apparent vascular amyloid deposition was detected in WT mice. However, cortical CAA was observed in APP/PS1/LV-GFP mice, which was significantly downregulated by LV-KL (Figure 2e,f).

The current findings showed that Klotho overexpression decreased A β burden in AD mice. Notably, consistent with the previously reported interactions between cerebral blood flow (CBF) reductions and aberrant vascular A β deposition, we observed a significant reduction of CBF in APP/PS1/LV-GFP mice compared with WT/LV-GFP mice, and this reduction was significantly reversed by LV-KL (Figure 2g).

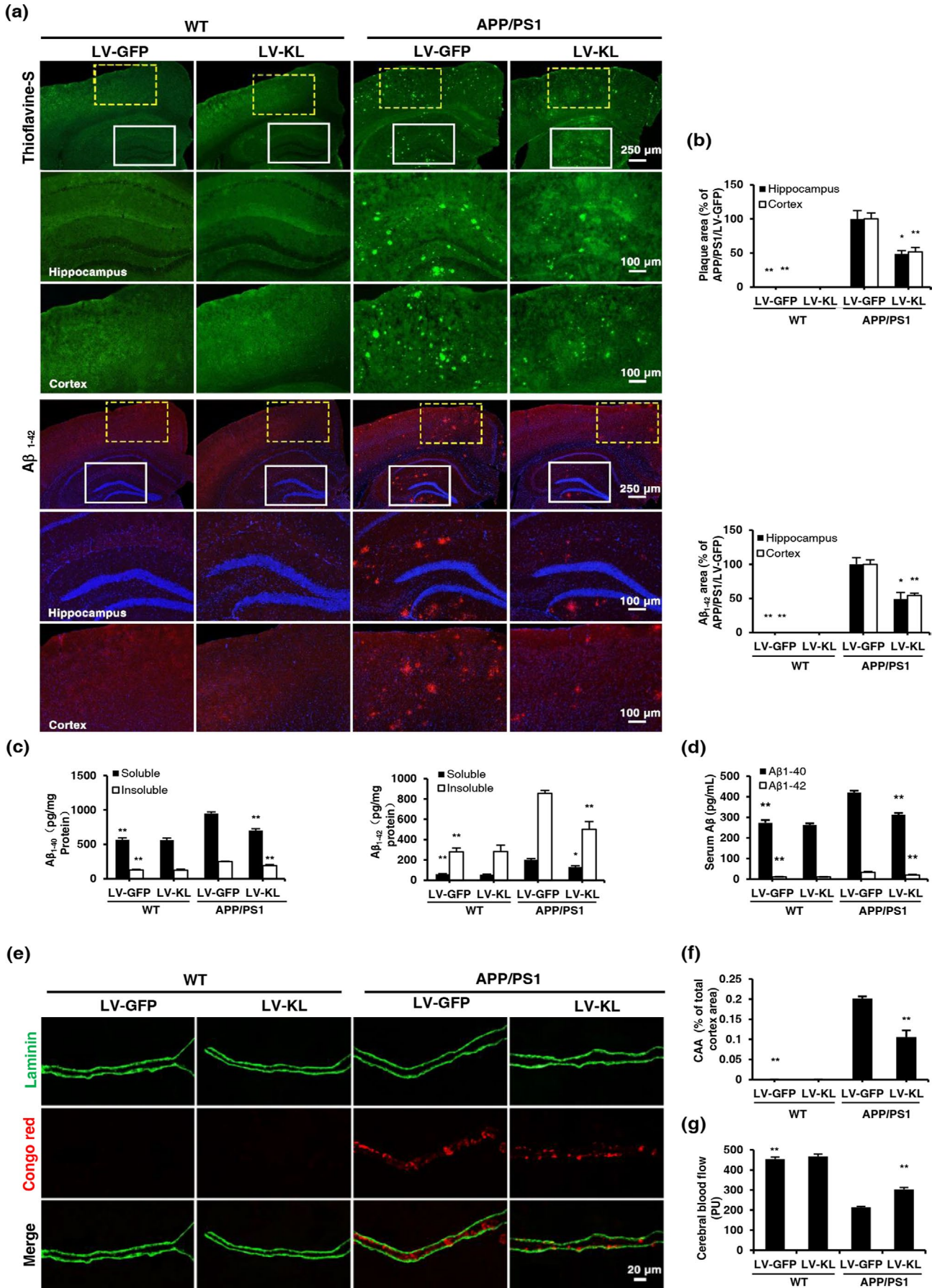
2.3 | Klotho overexpression ameliorated neuronal injury in the brain in aged APP/PS1 mice

Amyloid- β is highly neurotoxic, which may result in cerebral neuronal injury *in vivo*. In the present study, we observed approximately 30% and 50% neuronal loss in the hippocampal CA1 area and cortex, respectively, in APP/PS1/LV-GFP mice compared with WT/LV-GFP mice, while LV-KL significantly preserved neuronal survival in APP/PS1 mice (Figure 3a-c). In addition, significantly reduced synaptophysin (SYN) level was observed in the hippocampus CA1 area and cortex in APP/PS1/LV-GFP mice compared with WT/LV-GFP mice, which was significantly rescued by LV-KL (Figure 3a,d). The current findings showed that Klotho overexpression ameliorated neuronal and synaptic loss in AD mice.

2.4 | Klotho overexpression promoted microglial transformation and inhibited tau pathology in the brain in aged APP/PS1 mice

Studies have shown that A β activates the NLRP3 inflammasome. We examined activation of the NLRP3/caspase-1 signaling pathway in the brain in APP/PS1 mice. Western blotting showed that the expression of NLRP3, apoptosis-associated speck-like protein (ASC), and cleaved caspase-1 significantly increased in the brain in APP/PS1/LV-GFP mice compared with WT/LV-GFP controls (Figure 4a,b), and these increases were significantly reversed by LV-KL. The mRNA and protein levels of interleukin-1 β (IL-1 β), the final product of the NLRP3/caspase-1 signaling pathway, also significantly increased in APP/PS1 mice compared with WT mice, and this increase was reversed by LV-KL (Figure 4c). The current findings showed that Klotho overexpression inhibited activation of the NLRP3/caspase-1 signaling pathway. We also observed that LV-KL decreased tau phosphorylation, indicating that LV-KL improved tau pathology (Figure 4d).

FIGURE 2 Klotho overexpression reduced A β burden in aged APP/PS1 mice. (a) The distribution of amyloid plaques was detected using Thioflavine-S staining and A β_{1-42} monoclonal antibody in the hippocampus and cortex. (b) Quantitative image analysis of amyloid plaque accumulation based on Thioflavine-S-positive and A β_{1-42} -positive fluorescence area in the hippocampus and cortex. The data are expressed as each normalized value relative to the APP/PS1/LV-GFP group. (c) Levels of soluble and insoluble A β_{1-40} and A β_{1-42} in brain homogenates, measured by ELISA. (d) Serum levels of A β_{1-40} and A β_{1-42} , measured by ELISA. (e) Representative images of cerebral amyloid angiopathy (CAA), revealed by double-stained vessels (Laminin, green; aggregated A β peptide, Congo red). (f) Quantitative image analysis of CAA load in the total cerebral cortex area. (g) Cerebral blood flow (CBF) in the cortex. $n = 6$ /group, except $n = 12$ in (g). The data are expressed as mean \pm SEM. The statistical analysis was performed using two-way ANOVA followed by the Bonferroni-Holm post hoc test. * $p < 0.05$, ** $p < 0.01$, vs. APP/PS1/LV-GFP group

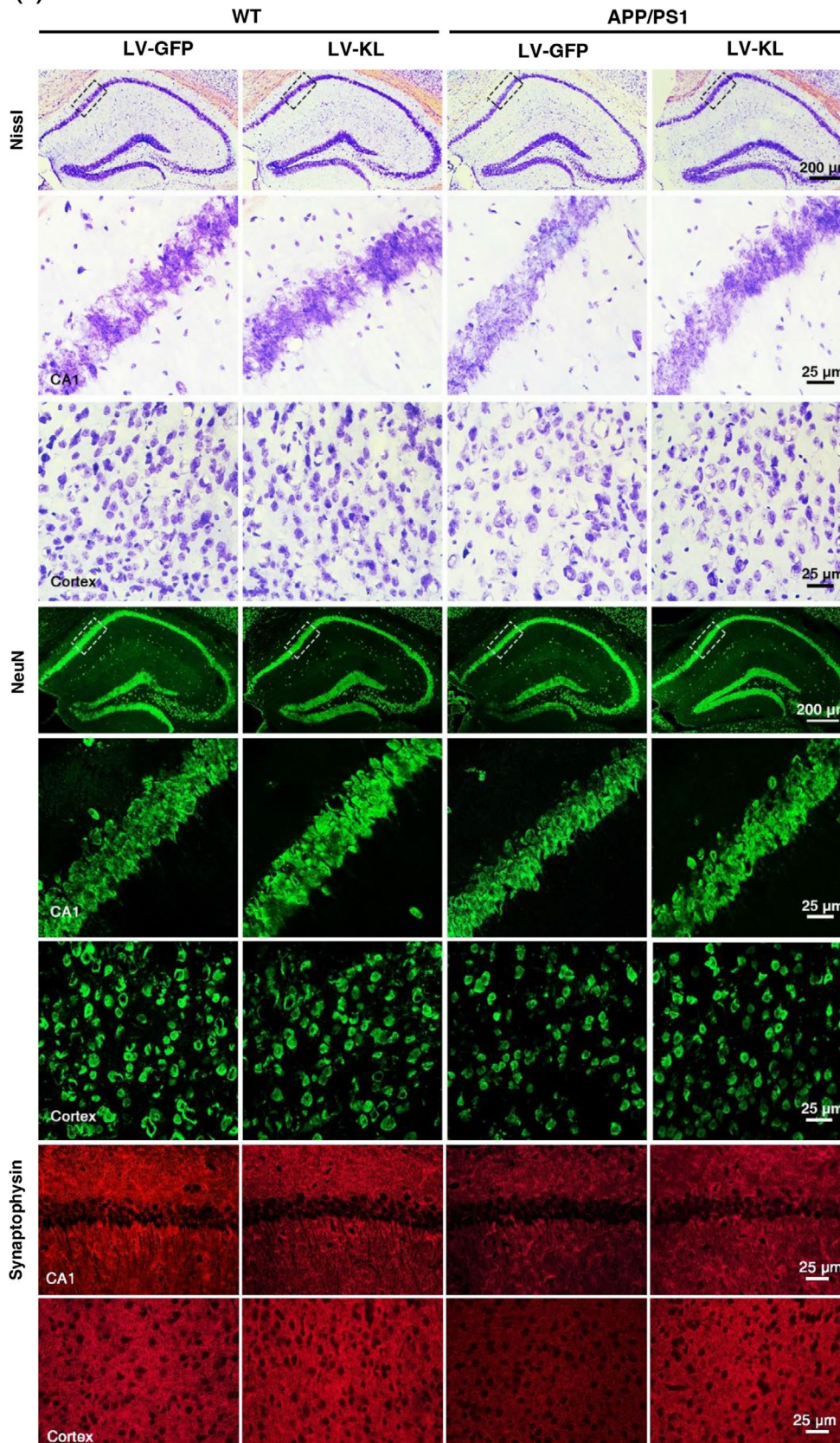




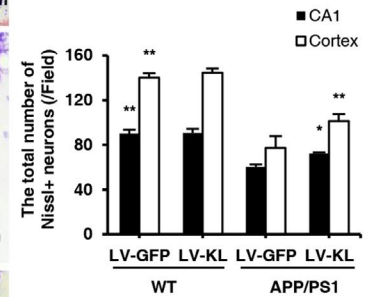
Microglia are highly plastic and can switch between the classic activated M1 type and substitutively activated M2 type. The NLRP3/caspase-1 signaling pathway is one of the main pathways

that regulate microglial activation and transformation. Studies have shown that the NLRP3 inflammasome promotes the transformation of microglia from the M2 type to M1 type, triggering an inflammatory

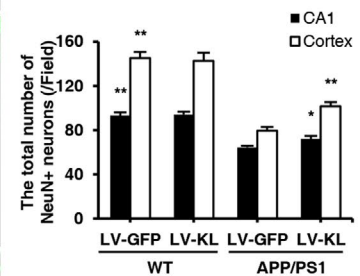
(a)



(b)



(c)



(d)

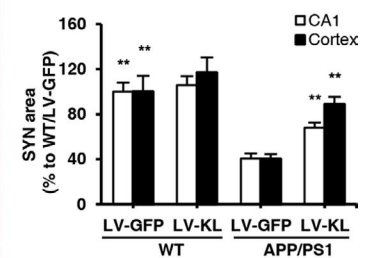


FIGURE 3 Klotho overexpression alleviated neuronal injury in the brain in aged APP/PS1 mice. (a) Representative images of Nissl staining, NeuN, and synaptophysin immunofluorescent staining in the hippocampal CA1 area and cortex. (b) Quantitative analysis of the number of Nissl-positive neurons in the hippocampal CA1 area and cortex. (c) Quantitative analysis of the number of NeuN-positive neurons in the hippocampal CA1 area and cortex. (d) Quantitative analysis of the synaptophysin (SYN)-positive area in the hippocampal CA1 area and cortex. $n = 6/\text{group}$. The data are expressed as mean \pm SEM. The statistical analysis was performed using two-way ANOVA followed by the Bonferroni-Holm post hoc test. $**p < 0.01$, vs. APP/PS1/LV-GFP group

response and reducing the clearance of A β . Therefore, we detected the surface antigens CD86 and CD206 of these two phenotypes in microglia. APP/PS1/LV-GFP mice exhibited more than a two-fold increase in the CD86-to-Iba-1 ratio and an approximately 50% decrease in the CD206-to-Iba-1 ratio in the hippocampal CA1 area and cortex compared with WT/LV-GFP controls. Interestingly, LV-KL induced an approximately 30% decrease in the CD86-to-Iba-1 ratio and 90% increase in the CD206-to-Iba-1 ratio in the hippocampal CA1 area and cortex in APP/PS1 mice compared with WT/LV-GFP mice (Figure 4e,f).

The current findings showed that Klotho overexpression promoted the transformation of microglia from the M1 type to M2 type in AD mice, which was associated with inhibition of the NLRP3/caspase-1 signaling pathway.

2.5 | Klotho overexpression affected the expression of A β transporters in aged APP/PS1 mice

The continuous clearance of A β from the central nervous system is vital for preventing its accumulation. Transport from the brain to the blood through the BBB and blood-CSF barrier primarily accounts for the clearance of total A β . LRP1 and P-gp might act in a coordinated fashion to traffic A β peptides from the brain into systemic circulation. Additionally, RAGE was shown to transport A β peptides back into the ISF (Xin, Tan, Cao, Yu, & Tan, 2018). In the present study, LRP1 and P-gp protein levels significantly decreased and ABCA1 and RAGE protein levels significantly increased in lectin-positive endothelial cells in the cortex and choroid plexus in APP/PS1/LV-GFP mice compared with WT/LV-GFP mice, which were reversed by Klotho treatment (Figure 5a,b). The mRNA and protein levels of LRP1 and P-gp were upregulated, and ABCA1 and RAGE levels were downregulated by LV-KL in brain homogenates in APP/PS1 mice (Figure 5c,d).

The current findings showed that Klotho overexpression regulated the expression of A β transporters. Notably, Klotho overexpression enhanced the level of soluble LRP1 (sLRP1) in serum of APP/PS1 mice (Figure 5e).

2.6 | Klotho knockdown decreased A β transport across the human blood-CSF barrier in an in vitro model and regulated the expression of A β transporters in HCPEpiCs

To further investigate the involvement of Klotho in A β trafficking at the blood-CSF barrier, we silenced Klotho in HCPEpiCs by

infecting these cells with a lentivirus that expressed shRNA that targeted Klotho mRNA at 1414–1442 bp (shKlotho; Figure 6a), which significantly reduced Klotho expression by approximately 77.4% (Figure 6b,c). We then constructed an in vitro model of the blood-CSF barrier by culturing a single monolayer of HCPEpiCs on inserts with collagen-coated transwell membrane filters (Figure 6d). Consistent with previous studies (Kuplennik, Lang, Steinfeld, & Sosnik, 2019), our blood-CSF barrier model had a high TEER value ($>30 \Omega \cdot \text{cm}^2$) and a low permeability constant ($5.19 \pm 1.23 \cdot 10^{-7} \text{ cm/s}$) to rhodamine B (RB)-labeled dextran, indicating a relatively impermeable monolayer (Figure 6e,f). The A β_{1-42} transport analysis showed that shKlotho significantly decreased Papp_{A-B}, increased Papp_{B-A}, and decreased the rate of efflux of soluble FITC-A β_{1-42} (Figure 6g,h), suggesting that Klotho knockdown impeded A β clearance across the human blood-CSF barrier.

Next, we investigated whether the reduction of A β efflux across the blood-CSF barrier by Klotho knockdown was associated with alterations of A β transporter levels. We examined mRNA levels of transporters in each group. We observed significant decreases in LRP1 and P-gp mRNA levels and significant increases in ABCA1 and RAGE mRNA levels in the shKlotho group compared with the shNC group (Figure 6i). The current findings showed that Klotho knockdown inhibited A β transport across the blood-CSF barrier by regulating the expression of its transporters in choroid plexus epithelial cells.

3 | DISCUSSION

Klotho was initially described as an anti-aging gene. Previous studies showed that Klotho expression in the brain in AD patients and mouse models significantly decreased compared with age-matched control groups. Klotho overexpression has been shown to alleviate AD-like pathology and cognitive impairments in mouse models of AD (Dubal et al., 2015; Kuang et al., 2017; Massó et al., 2015; Semba et al., 2014). The present study used 7-month-old APP/PS1 mice, which developed early AD-relevant pathological deficits, and maintained Klotho overexpression for up to 6 months by lentivirus injections. Our data showed that Klotho overexpression attenuated AD pathology, which was consistent with our previous report (Zeng et al., 2019). We found that Klotho overexpression significantly improved cognitive decline, reduced A β burden, ameliorated neuronal and synaptic loss, and increased CBF in APP/PS1 mice. These neuroprotective effects of Klotho appeared to be relevant to the promotion of the transformation of microglia from the M1 type to M2 type and the regulation of A β transporters, which increased the clearance of A β . Notably, we

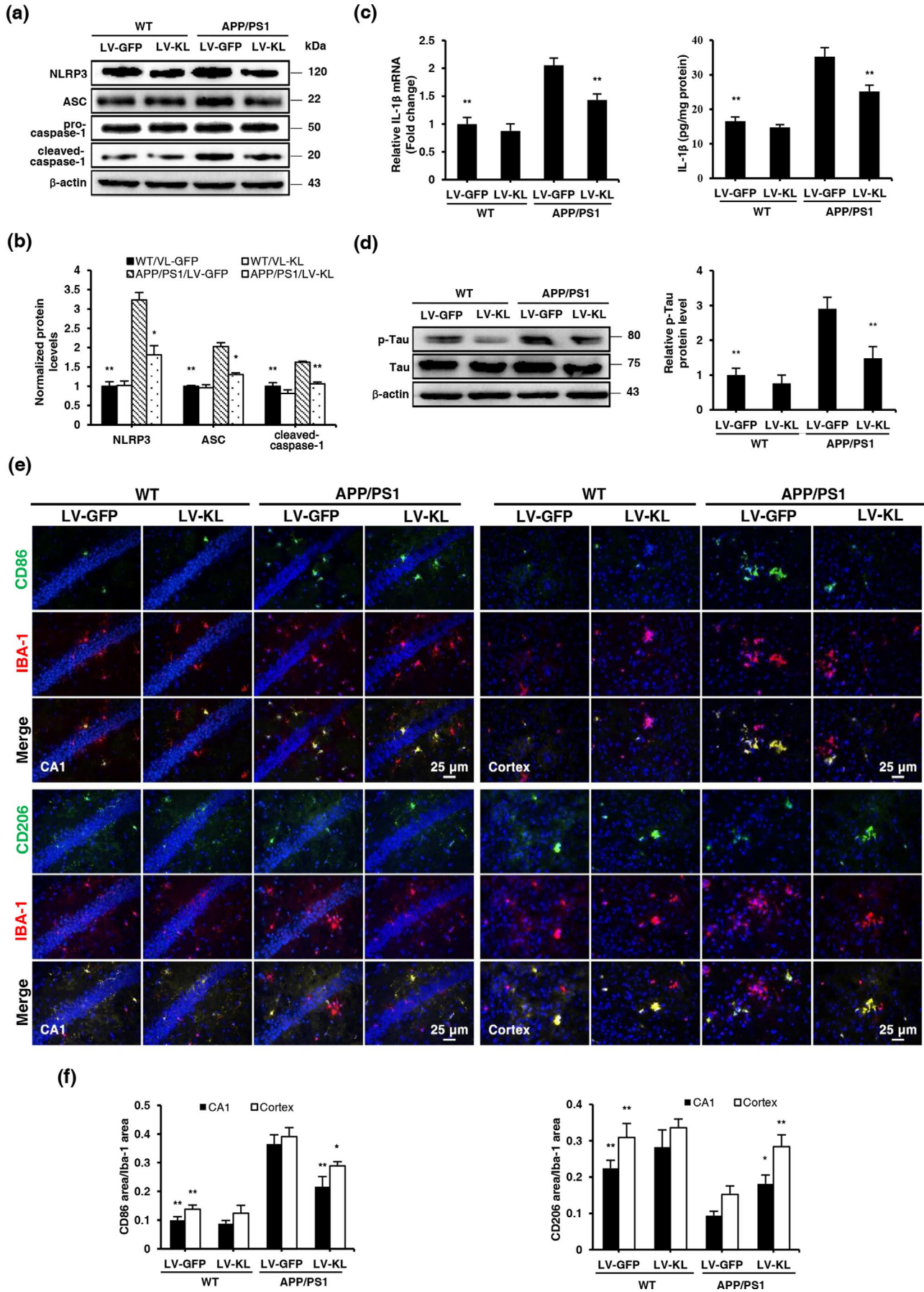


FIGURE 4 Klotho overexpression promoted microglial transformation and alleviated Tau pathology in the brain in aged APP/PS1 mice. (a, b) Representative Western blotting and quantification of NLRP3, ASC, cleaved caspase-1, and β -actin in brain tissues. The amount of NLRP3, ASC, and cleaved caspase-1 were normalized to β -actin. (c) Analyses of IL-1 β mRNA levels and protein concentrations in brain homogenates by qRT-PCR and ELISA, respectively. Relative mRNA levels of IL-1 β were normalized to GAPDH and are expressed as fold changes relative to the WT/LV-GFP group. (d) Representative Western blotting and quantification of p-Tau and Tau in brain tissues. The amount of p-Tau was normalized to Tau. (e) Representative images of CD86 and CD206 (green) counterstained with Iba-1 (red) and nuclear DNA staining of DAPI (blue) in the hippocampal CA1 area and cortex. (f) Quantitative image analysis of CD86/Iba-1 and CD206/Iba-1 expression based on positive fluorescence area in the hippocampal CA1 area and cerebral cortex. The data are expressed as each normalized value relative to the WT/LV-GFP group. $n = 6$ /group, except $n = 4$ /group in (a, b, d). The data are expressed as mean \pm SEM. The statistical analysis was performed using two-way ANOVA followed by the Bonferroni-Holm post hoc test. * $p < 0.05$, ** $p < 0.01$, vs. APP/PS1/LV-GFP group

did not observe similar effects in WT mice, suggesting that Klotho overexpression may have little effect in normal mice. However, we also observed that Klotho overexpression had no effect on the content of p53 in the brain of APP/PS1 mice (Figure S1), suggesting that Klotho upregulation does not affect the expression of other proteins, such as p53.

It is well known that A β -induced neurotoxic effects (neuronal and synaptic loss) are the potential causes of cognitive deficits in AD. A recent study published in *Molecular Psychiatry* indicates that the treatment with adipoRon (APN receptor agonist) might significantly lower A β levels, rescue neuronal and synaptic loss, and improve spatial memory functions in AD mice (Ng et al., 2020). SYN is an important indicator of synaptic density and synaptic formation. In the present study, i.c.v. injection of LV-KL increased NeuN and SYN immunoreactivity, and improved cognitive function in AD mice. Our results showed that treatment with Klotho might ameliorate A β -induced neuronal and synaptic loss, and cognitive deficits in mice. In addition, several studies have reported the effects of Klotho on synaptic plasticity. Dubal et al. (2014) found that elevating Klotho in mice might increase synaptic levels of the GluN2B subunit of NMDARs, enhance hippocampal LTP, and increase the GluN2B portion of NMDAR currents. Dubal et al. (2015) also showed that Klotho elevation in hAPP/KL mice increased NMDAR-dependent long-term potentiation (LTP) despite of not altering hippocampal levels of A β . Li et al. (2019) found that secreted human Klotho altered some synaptic plasticity-related proteins and mediated a significant increase in fEPSP slope per unit of stimulation intensity in mice. These results showed the direct regulation of Klotho itself on synaptic plasticity in mice. The further investigation is required to elucidate the underlying mechanism of Klotho in the future.

A β is an NLRP3 inflammasome activator. Numerous studies have shown that the NLRP3 inflammasome plays an important role in the pathogenesis of AD (Saresella et al., 2016; Yin et al., 2018). Consistent with previous studies (Zhu, Stein, et al., 2018), we observed significant increases in the expression of NLRP3, ASC, and cleaved caspase-1 in the brain in APP/PS1 mice compared with WT mice, which were reversed by LV-KL. Klotho overexpression also significantly inhibited the expression of IL-1 β , a product of the activation of NLRP3/caspase-1 signaling pathway. These results indicated the inhibition of the NLRP3/caspase-1 pathway by Klotho overexpression. Interestingly, a recent study reported that NLRP3 activation by A β rather than A β itself was closely related to tau phosphorylation (Ising et al., 2019). In the present study, we also found a

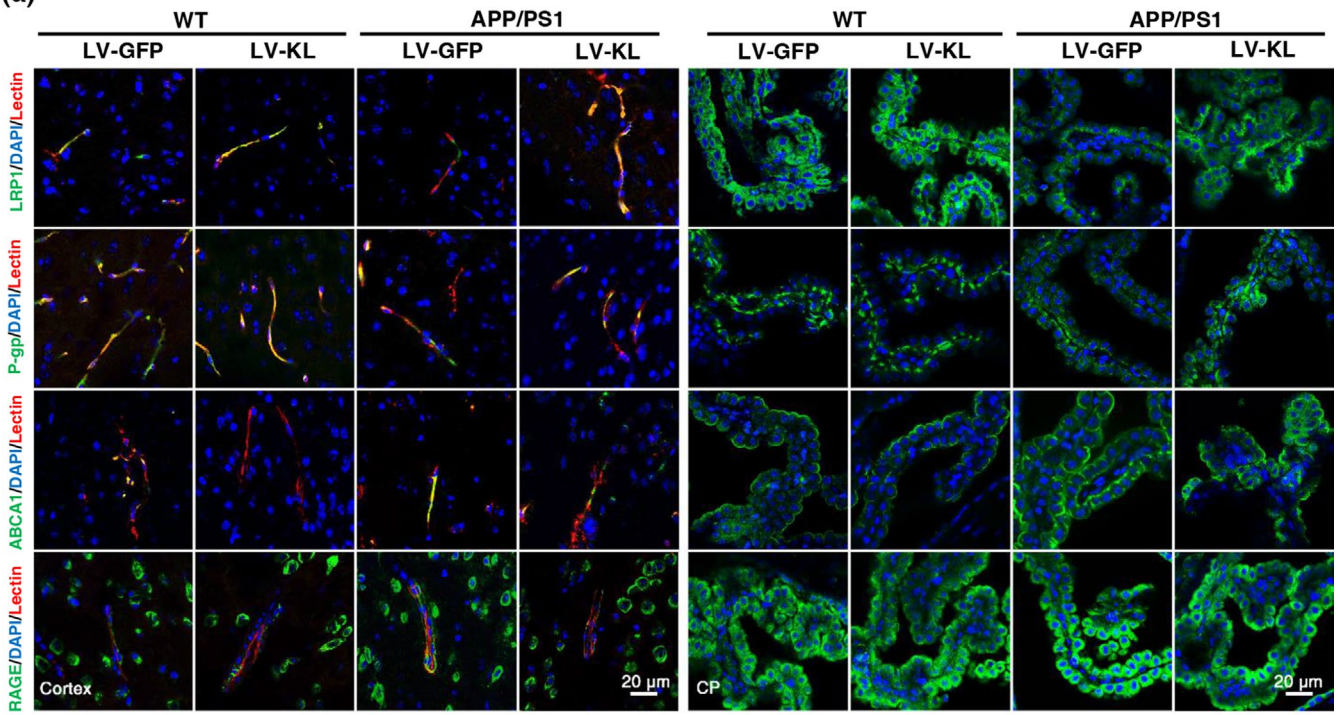
decrease in tau phosphorylation levels in the brain in APP/PS1 mice with Klotho overexpression.

Promoting the clearance of A β is an important topic in AD research. A β clearance in the central nervous system is a complex process that is mediated by various systems and cell types, including the ubiquitin-proteasome system, autophagy-lysosome, proteases, microglial phagocytosis, glymphatic drainage and transport to the periphery via the BBB, arachnoid villi, and the blood-CSF barrier (Xin et al., 2018). Our previous study focused on the impact of Klotho overexpression on the degradation of autophagy for A β clearance (Zeng et al., 2019). However, whether Klotho overexpression also affects other pathways remains unclear. Previous studies showed that the inhibition of NLRP3 inflammasome promoted the transformation of microglia to M2 type and enhanced the clearance of A β as well as spatial memory in AD mice (Heneka et al., 2013). Since Klotho can reduce NLRP3/caspase-1 signaling pathway, we speculated that Klotho can promote the transformation of microglia to M2 type. Consistent with the conjecture, we observed that the overexpression of Klotho increased the expression of CD206 in the hippocampal CA1 area and cortex of APP/PS1 mice, which is the surface antigen of M2-type microglia. In general, the present findings showed that Klotho overexpression promoted the transformation of microglia in APP/PS1 mice from the M1 type to M2 type, thereby increasing the clearance of A β by microglia in AD mice.

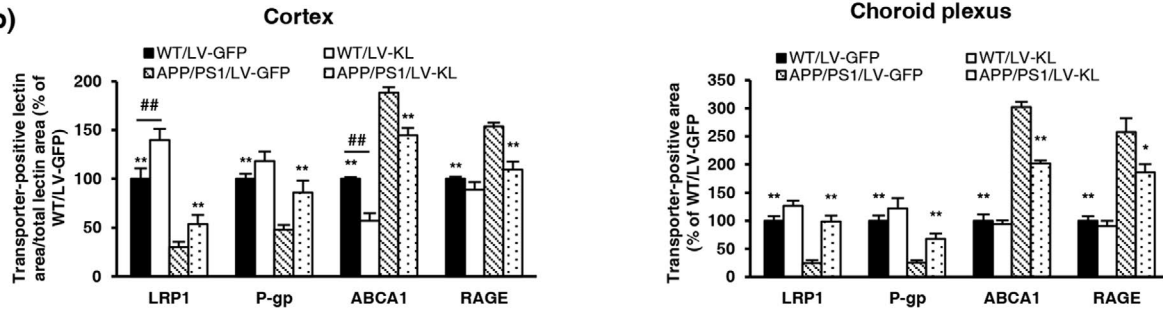
In addition to microglial phagocytosis, A β trafficking from the brain to blood by transporters at the BBB plays an important role in reducing A β levels in the brain (Xin et al., 2018). Cross-talk among transporters, including LRP1 and P-gp, plays a critical role in promoting A β clearance from the brain to blood (EIALi & Rivest, 2013), and RAGE mediates the influx of A β back into the brain (Cai et al., 2016). Consistent with previous articles (Chiu et al., 2015), we found that LRP1 and P-gp expression decreased, and RAGE expression increased in the BBB and cerebrum in APP/PS1 mice. Our results showed that Klotho overexpression restored the aberrant levels of these transporters. Klotho overexpression induced the expression of LRP1 and P-gp, suggesting upregulation of the transcytosis of A β peptide across the BBB from the brain to blood. The reduction of RAGE expression suggested suppression of the influx of A β peptide across the BBB from the blood to brain. Collectively, our findings indicated that Klotho overexpression upregulated A β clearance across the BBB. Notably, we also found that Klotho overexpression decreased the expression of ABCA1 in the BBB and brain in AD mice. ABCA1 has been reported to facilitate A β elimination



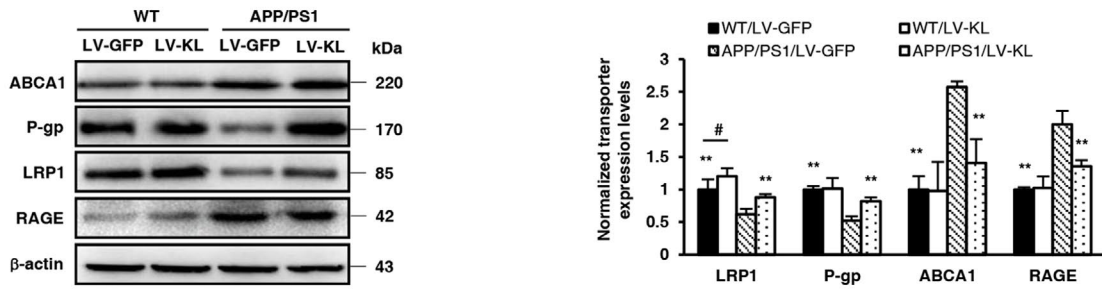
(a)



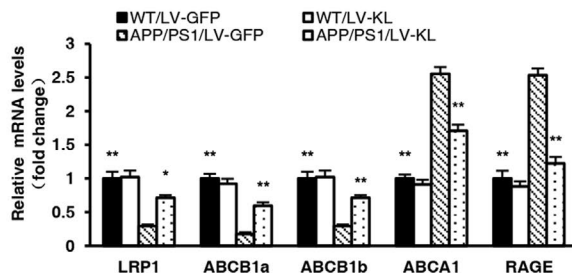
(b)



(c)



(d)



(e)

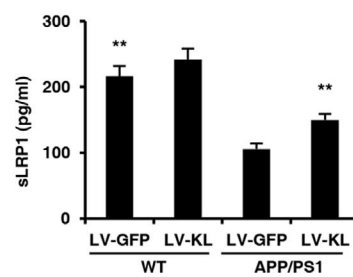




FIGURE 5 Klotho overexpression affected the expression levels of A β transporters in aged APP/PS1 mice. (a) Representative immunofluorescence images of A β transporters (green) in the cortex (left) and choroid plexus (right), including low-density lipoprotein receptor-related protein 1 (LRP1), P-glycoprotein (P-gp), ATP-binding cassette transporter A1 (ABCA1), and receptor for advanced glycation end products (RAGE). The lectin-positive area (red) indicates micro-vessels. Nuclei were stained with DAPI (blue). (b) Quantitative analysis of the levels of A β transporters in micro-vessels and the choroid plexus. (c) Representative Western blotting and quantification of the relative protein levels of LRP1, P-gp, ABCA1, and RAGE in brain tissue homogenates. Protein levels were normalized to GAPDH and are expressed as fold changes relative to the WT/LV-GFP group. (d) Analyses of LRP1, P-gp, ABCA1, and RAGE mRNA levels in brain tissue homogenates by qRT-PCR. Relative mRNA levels were normalized to GAPDH and are expressed as fold changes relative to the WT/LV-GFP group. (e) Soluble LRP1 (sLRP1) levels in serum, measured by ELISA. $n = 6$ /group, except $n = 4$ /group in (c). The data are expressed as mean \pm SEM. The statistical analysis was performed using two-way ANOVA followed by the Bonferroni-Holm post hoc test. * $p < 0.05$, ** $p < 0.01$, vs. APP/PS1/LV-GFP group; # $p < 0.05$, ## $p < 0.01$, vs. WT/LV-GFP group

in an ApoE-dependent manner, and ApoE lipidation may competes for LRP1, blocking A β clearance (EIAli & Rivest, 2013; Martiskainen et al., 2013). In the present study, we did not investigate ApoE. Whether the LRP1-mediated transport of ApoE-bound A β is affected by Klotho overexpression is unknown.

The sLRP1 is a cleavage product of LRP1 that sequesters A β in the periphery and mediates its clearance in the liver. It has been reported that sLRP1 can prevent the access of A β to RAGE and RAGE-mediated A β influx (Wang, Gu, Masters, & Wang, 2017). To further investigate whether alterations of serum A β levels were related to disturbances in periphery transport, we measured circulating sLRP1 levels. We found that serum sLRP1 levels significantly decreased in APP/PS1 mice, which was reversed by Klotho. The upregulation of sLRP1 by Klotho would further enhance peripheral A β sequestration, thereby promoting A β clearance in the periphery.

A β in the brain is mainly removed by efflux across the BBB, and A β in the extracellular space of the brain can enter CSF freely. A β in CSF can be absorbed into the circulation via spinal arachnoid villi or the blood-CSF barrier, and the blood-CSF barrier is the primary channel for A β removal (Xin et al., 2018). Capillaries in the choroid plexus are highly fenestrated. The blood-CSF barrier is formed by choroid plexus epithelial cells (CPECs) and separates blood from CSF. Additionally, CPECs contain many specific transporters that confer an active role in the regulation of transport between the blood and CSF (Erickson & Banks, 2013). In the present study, we observed the distribution of these transporters by immunofluorescence microscopy. We found that LRP1 and RAGE moved between the cytosol and external limiting membranes of the choroid plexus. ABCA1 was clearly localized to the outer edge of the choroid plexus, whereas P-gp was expressed at the basolateral membrane of CPECs. These findings suggested that transport/distribution principles of transporters at the BBB were also applicable to the blood-CSF barrier in removing A β from CSF. We observed decreases in expression of the efflux transporters LRP1 and P-gp and increases in the expression of ABCA1 and RAGE at the blood-CSF barrier in 13-month-old APP/PS1 mice, suggesting that compensatory A β clearance via the blood-CSF barrier failed similarly to failure at the BBB. Together, our findings suggested that Klotho overexpression promoted A β clearance across the blood-CSF barrier by increasing LRP1 and P-gp expression and decreasing RAGE and ABCA1 expression in the choroid plexus in APP/PS1 mice.

The results of our in vitro model of the human blood-CSF barrier also directly showed that Klotho facilitated A β efflux across the blood-CSF barrier by regulating transporter levels. We found that Klotho knockdown in the in vitro blood-CSF barrier model significantly decreased the transepithelial permeability of soluble A β_{1-42} from the CSF side to blood side but increased its permeability from the blood side to CSF side, suggesting that Klotho promoted A β clearance from the blood-CSF barrier. Klotho knockdown also decreased LRP1 and P-gp mRNA levels but increased ABCA1 and RAGE mRNA levels in HCPEpiCs, consistent with the in vivo results. Overall, our results provided evidence that Klotho plays a role in A β clearance by regulating A β transporters at the blood-CSF barrier. The production of CSF and integrity of the blood-CSF barrier were also shown to play important roles in A β clearance. Dysfunction of the choroid plexus, together with compromised CSF production (Chiu et al., 2012), diminishes the clearance of A β peptide, indicating its involvement in AD pathology (Serot et al., 2011; Silverberg et al., 2010). In the present study, we did not observe significant effects of Klotho knockdown on blood-CSF barrier integrity, reflected by no changes in TEER or dextran permeability.

In summary, the present study found that Klotho overexpression inhibited NLRP3 inflammasome activation and promoted A β clearance through an increase in M2 type microglia and the regulation of A β transporters in APP/PS1 mice, which effectively relieved neuroinflammation and A β burden and ameliorated AD-like phenotypes. Moreover, Klotho knockdown reduced the transporter-mediated efflux rate of soluble A β_{1-42} across the blood-CSF barrier in an in vitro monolayer model. Our findings indicate that Klotho overexpression in the central nervous system may be a potential strategy for the treatment of AD.

4 | EXPERIMENTAL PROCEDURES

4.1 | Cell cultures

HCPEpiCs were obtained from ScienCell Research Laboratories and cultured in epithelial cell medium according to the distributor's recommendations. HCPEpiCs at passages 3–5 were used for the experiments. HEK293 cells were purchased from Humanitas Clinical and Research Center (Rozzano, Milan, Italy) and cultured in Dulbecco's modified Eagle's medium supplemented with 10% fetal bovine serum.

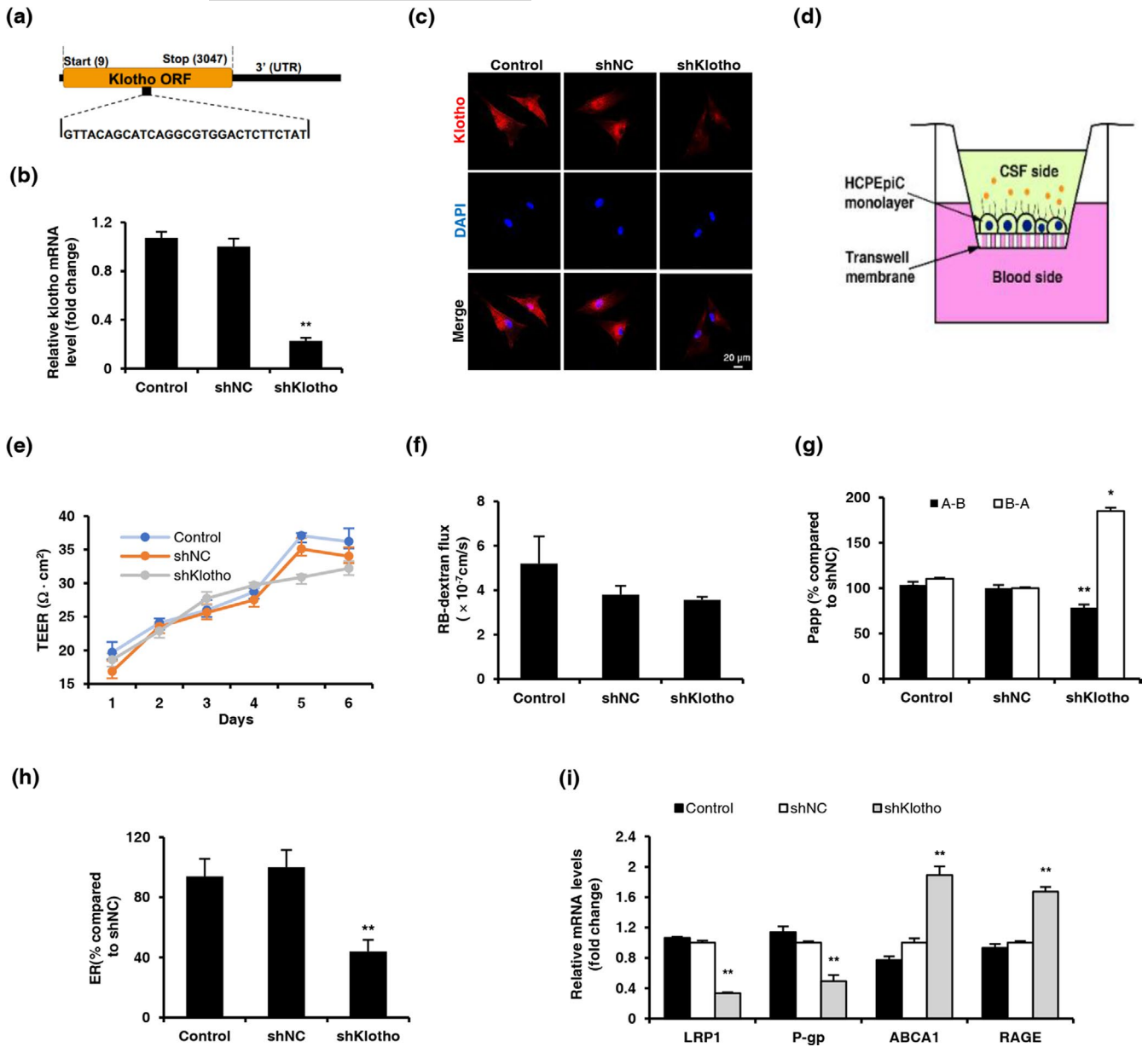


FIGURE 6 Klotho knockdown decreased the active transport of $\text{A}\beta$ across the human blood-CSF barrier in an in vitro model. (a) Schematic representation of the location of the shRNA target within the Klotho coding sequence (shKlotho). (b) Analysis of Klotho mRNA levels in primary human choroid plexus epithelial cells (HCPEpiCs) infected with shKlotho or shNC at a multiplicity of infection (MOI) of 80. Relative mRNA levels were normalized to β -actin and are expressed as fold changes relative to shNC-treated cells. (c) Representative confocal images of Klotho (red) in HCPEpiCs, examined by immunofluorescence 5 days after infection. Nuclear DNA was stained with DAPI (blue). (d) Paradigm for the in vitro model of the human blood-cerebrospinal fluid barrier (BCSFB), consisting of a monolayer of HCPEpiCs. (e) Transepithelial electrical resistance (TEER) measured after seeding across the BCSFB monolayer. (f) Permeability of HCPEpiCs monolayer to 1 mg/ml RB-dextran. (g) Bidirectional transfer of 0.5 μM FITC- $\text{A}\beta_{1-42}$ across the BCSFB monolayer from the basolateral to apical side (B \rightarrow A) and from the apical to basolateral side (A \rightarrow B). (h) FITC- $\text{A}\beta_{1-42}$ efflux rate across the BCSFB monolayer. The data were normalized to shNC-treated cells. (i) Analyses of LRP1, P-gp, ABCA1, and RAGE mRNA levels in primary human choroid plexus epithelial cells by qRT-PCR. The data were normalized to β -actin and are expressed as fold changes relative to shNC-treated cells. The data are from three independent experiments and are expressed as mean \pm SEM. * $p < 0.05$, ** $p < 0.01$, vs. shNC-treated cells. Cells that were incubated in epithelial cell medium without vectors were used as the normal control. The statistical analysis was performed using one-way ANOVA followed by the LSD test. Kruskal-Wallis test was used when variance was uneven

4.2 | Animals

Male 6.5-month-old $\text{APP}^{\text{Swe}}/\text{PS1}^{\text{DE9}}$ transgenic mice (Beijing HFK Bioscience Co. Ltd) and WT mice both on C57BL/6 background were used

in this study. All treatments were approved by the ethics committee of the University of Sichuan (number K2018085). All studies were carried out in accordance with the Regulations of Experimental Animal Administration promulgated by the State Committee of Science and Technology of China.



4.3 | Plasmid and lentivirus preparation

Green fluorescent protein (GFP)-tagged lentiviral plasmid carrying a full-length mouse *Klotho* cDNA (LV-KL) or shRNA against human *Klotho* (shKlotho) were purchased from OriGene Technologies, supplemented with a negative control (LV-GFP or shNC, respectively). The mouse lentiviral particles were subsequently packaged as we previously reported (Zeng et al., 2019). The shRNA lentiviral particles were packaged by GeneChem Company.

4.4 | Lentivirus administration

Seven-month-old mice were randomly divided into four groups: APP/PS1/LV-GFP, APP/PS1/LV-KL, WT/LV-GFP, and WT/LV-KL ($n = 12$ per group). Then, a bilateral intracerebroventricular (i.c.v.) injection of corresponding LV-KL or LV-GFP (3 μ l per side, 4.10×10^7 TU/ml) was conducted as reported previously. Three months later, one additional injection of lentivirus was given in the same way.

4.5 | Neurobehavioral tests

The Y-maze test was carried out on the last day of each month after i.c.v. injection. The passive avoidance test and Morris water maze test were conducted 3 months after supplemental injection. All the neurobehavioral tests were performed as we previously reported (Zeng et al., 2019).

4.6 | Cerebral blood flow measurement

One day after Morris water maze test, the mice were anesthetized and fixed, and cerebral blood flow (CBF) in the cortex was measured by MoorVMS laser Doppler perfusion (Moor Instruments Ltd) as we previously described (Zeng et al., 2019).

4.7 | Tissue and blood collection

After CBF measurement, blood was collected from orbital sinus immediately for serum separation. Followed by transcardially perfused with cold saline, the brains were rapidly removed and split into two hemispheres. The right hemisphere was frozen for 20-micron-thick sections, while the left hemisphere was homogenized for biochemical analysis without choroid plexus.

4.8 | Histological evaluation

The in situ hybridization (ISH) analysis, immunohistochemistry (IHC) analysis and immunofluorescence (IF) analysis were performed as we previously reported (Zeng et al., 2019). Negative control sections were

processed by omitting the complementary RNA or primary antibody. Nissl staining (0.5% cresyl violet) and Congo red staining (0.5% Congo red) were performed the same as previous studies (Zeng et al., 2019). For Thioflavine-S staining, the slides were incubated with 0.05% Thioflavine-S (Sigma) and then differentiated in 80% ethanol solution. Each section containing one microscopic field of the choroid plexus was digitized using a 40 \times objective. The total area of CAA was analyzed as percentage of total cortex area, and seven different sections from each mouse were determined in CAA. For other histological evaluation, three microscopic fields in hippocampus or cortex of each section were examined, respectively. All slides were mounted and imaged on a Nikon microscope or ZEISS LSM800. IF analysis of cultured cells was performed in the same way as tissue sections. The primary antibodies we used were showed in Table 1.

4.9 | Quantitative real-time polymerase chain reactions

Total RNA was isolated using TRIzol reagent (Invitrogen) and cDNA was generated using RevertAid First Strand cDNA Synthesis kit (Thermo). The optimized primer sequences were synthesized by Beijing Genomics Institute (Table 2). Quantitative real-time polymerase chain reactions (qRT-PCR) was carried out as we previously reported (Zeng et al., 2019). The results were normalized to GAPDH using the $2^{-\Delta\Delta CT}$ method.

4.10 | Enzyme-linked immunosorbent assay

The levels of $A\beta_{1-40}$, $A\beta_{1-42}$, IL-1 β , TNF- α , and *Klotho* were measured by ELISA kit (Cusabio Biotechnology) as we described previously (Zeng et al., 2019). The level of soluble LRP1 (sLRP1) in serum was examined using an ELISA kit (USCN Life Sciences) according to the manufacturers' instructions.

4.11 | Western blotting

The total proteins were extracted by RIPA buffer (Beyotime). Equal amounts of protein samples were separated by SDS-PAGE and then transferred to a PVDF membrane (Millipore) as we described previously (Zeng et al., 2019). The primary antibodies we used were shown in Table 1.

4.12 | Cell transfection

Klotho knockdown in HCPEpiCs was achieved by infection with the lentivirus (shNC, 8×10^7 TU/ml, shKlotho, 6×10^7 TU/ml) at a multiplicity of infection (MOI) of 80. HitransG P (GeneChem Company) was used to increase the infection efficiency. 24 h after infection, the medium was refreshed. The cells were screened with puromycin (1 μ g/ml) for 1 week and harvested to examine the *Klotho* mRNA and protein levels.



Antibody	Application	Dilution rate	Source	Catalog number
Klotho	IHC	1:200	Abcam, UK	ab181373
Klotho	ICC/IF	1:100	Santa Cruz, USA	sc-515939
NeuN	IF	1:100	Abcam, UK	ab177487
SYN	IF	1:100	Santa Cruz, USA	sc-17750
A β ₁₋₄₂	IF	1:200	Abcam, UK	ab201060
Laminin	IF	1:100	Abcam, UK	ab11757
Iba-1	IF	1:500	Wako, Japan	019-19741
CD86	IF	1:50	Abcam, UK	ab119857
CD206	IF	1:50	Abcam, UK	ab8918
NLRP3	WB	1:1000	AdipoGen, USA	AG-20B-0014-C100
Caspase-1	WB	1:1000	AdipoGen, USA	AG-20B-0044-C100
ASC	WB	1:1000	Wanlei, China	WL02462
LRP1	WB, IF	1:100	Abcam, UK	ab28320
RAGE	WB, IF	1:200	Santa Cruz, USA	sc-365154
ABCA1	WB, IF	1:200	Novus, USA	NB400-105S
P-gp	WB, IF	1:100	Santa Cruz, USA	sc-55510
Lectin	IF	1:100	Vector Laboratories, USA	DL-1177
Tau	WB	1:1000	Abcam, UK	Ab80579
p-Tau	WB	1:1000	CST, USA	#9632
β -actin	WB	1:1000	Zhongshanjinqiao, China	TA-09

Abbreviations: IF, Immunofluorescence; IHC, Immunohistochemistry; WB, Western blotting.

TABLE 1 Primary antibodies used in this study

Gene	Primer sequence forward (5'-3')	Primer sequence reverse (5'-3')
<i>Mouse GAPDH</i>	AGCGAGACCCCACTAACATC	GGTTCACACCCATCACAAAC
<i>Mouse IL-1β</i>	TTCAAATCTCGCAGCAGCAC	GTGCAGTTGTCTAATGGGAACG
<i>Mouse Klotho</i>	GGCTTTCTCTTTTACCTGAAAA	CACATCCCACAGATAGACATTCG
<i>Mouse LRP1</i>	CCGACTGGCGAACAATAACAC	ATCGGCTTTGTTGCACGTG
<i>Mouse RAGE</i>	AAAACGACAACCCAGGCGT	ATTCTCTGGCATCTCCGCTTC
<i>Mouse ABCA1</i>	GCCTGGATCTACTCTGTCTGC	GCCATTGTCCAGACCCATGA
<i>Mouse ABCB1a</i>	CATTGCGATAGCAGGAGTGG	CACCAAGTAGGCACCGAACC
<i>Mouse ABCB1b</i>	CTGGTATGGGACATCCTTGGT	CTGTCTGGTTGTAGCCCTTTG
<i>Human β-actin</i>	ACGAGGCCAGAGCAAGAG	GGTGTGGTGCCAGATCTTCTC
<i>Human klotho</i>	GCTCTCAAAGCCCACATACTG	GCAGCATAACGATAGAGGCC
<i>Human LRP1</i>	ACGAGGCCAGAGCAAGAG	GGTGTGGTGCCAGATCTTCTC
<i>Human RAGE</i>	GTGCTCTCCCAACGGCTC	ATTGCCTGGCACCGAAAA
<i>Human ABCA1</i>	GAAGTGGCTGTGTCCATGAT	GATGAGCCAGACTTCTGTTGC
<i>Human P-gp</i>	GCTCTGACTATGCCAAAGC	TCTTCACCTCCAGGCTCAGT

TABLE 2 Nucleotide sequences of primers used for the quantitative real-time PCR experiments

4.13 | Establishment of in vitro model of human BCSFB

The model was constructed with some modification following a protocol previously established (Dinner et al., 2016; Zheng & Zhao, 2002). Briefly, normal and lentivirus infected HCPEpiCs (1×10^5 cells/well) were seeded on the lower side of 24-well collagen-coated transwell membrane filter (Corning), respectively. 48 h later, the medium was refreshed every day.

4.14 | Transepithelial electrical resistance analysis

The barrier forming capacity of HCPEpiCs was evaluated by measuring the transepithelial electrical resistance (TEER) values using Millicell-ERS (Millipore) for consecutive 6 days after seeded. The TEER value of the HCPEpiCs monolayer was obtained as previously reported (Dinner et al., 2016). Cell layers showing TEER values between 30 and 40 $\Omega \cdot \text{cm}^2$ were used for the following experiments.



4.15 | Paracellular permeability analysis

The permeability of HCPEpiCs monolayer was determined as described with some modification (Zhu, Su, Fu, & Xu, 2018). Briefly, the medium in the upper chamber (apical side) was replaced with 200 μ l RB-dextran (40 kDa; Ruixi Biological Technology) solution (1 mg/ml) in Hank's balanced salt solution (HBSS), and the medium in the lower chamber (basolateral side) was replaced with 1000 μ l HBSS. 100 μ l samples were taken from the lower chamber at 10 min intervals for 120 min. While sampling each time, the lower chamber was replenished with equal volume of HBSS. The corresponding dextran concentrations were determined by measuring fluorescence intensity using a fluorescence plate reader (Thermo Scientific) at excitation/emission wavelength of 550 nm/620 nm. The permeability coefficients of RB-dextran across BCSFB monolayer was calculated as described (Zhu, Su, et al., 2018).

4.16 | Analysis of A β transport across the in vitro human BCSFB model

The transport of soluble A β ₁₋₄₂ across the BCSFB monolayer was tested in both directions [from the apical to the basolateral (A \rightarrow B) and from the basolateral to the apical (B \rightarrow A)] for 120 min. 0.5 μ M FITC-labeled A β ₁₋₄₂ (ChinaPeptides) was used in this experiment. Fluorescence intensity was measured at excitation/emission wavelength of 492 nm/520 nm. The apparent permeability coefficients and efflux rate of A β ₁₋₄₂ was quantified as described (Guo et al., 2016; Zhu, Su, et al., 2018).

4.17 | Statistical analysis

SPSS 20.0 software was used for the statistical analyses. Except that the alternation in Y-maze test and escape latency in Morris water maze test were analyzed using Mixed-design ANOVA with Bonferroni-Holm test, other in vivo data were analyzed using two-way ANOVA with Bonferroni-Holm test. The in vitro data were analyzed using one-way ANOVA with LSD's test. Kruskal-Wallis test was used when variance was uneven. Values of $p < 0.05$ were considered statistically significant.

ACKNOWLEDGEMENTS

This work was supported by the National Natural Science Foundation of China (81473219 and 81973307), 111 Project of the National Ministry of Education (B18035, China) and the Fundamental Research Funds for the Central Universities.

CONFLICT OF INTEREST

The authors declare no conflict of interests.

AUTHOR CONTRIBUTIONS

J-R Du conceptualized this study. J-R Du and X-H Li designed research. Y Zhao, C-Y Zeng, and T-T Yang performed research. Y Zhao

and C-Y Zeng analyzed data. X Kuang assisted in some acquisition of data. C-Y Zeng, Y Zhao, X-H Li, and J-R Du prepared the manuscript. J-R Du revised the manuscript.

DATA AVAILABILITY STATEMENT

The authors declare that the authors provide all data included in this study upon request when there is a reasonable request.

ORCID

Yue Zhao  <https://orcid.org/0000-0001-8676-4949>

REFERENCES

- Ahn, K. C., Learman, C. R., Dunbar, G. L., Maiti, P., Jang, W. C., Cha, H. C., & Song, M. S. (2018). Characterization of impaired cerebrovascular structure in APP/PS1 mouse brains. *Neuroscience*, *385*, 246–254. <https://doi.org/10.1016/j.neuroscience.2018.05.002>
- Baluchnejadmojarad, T., Eftekhari, S.-M., Jamali-Raeufy, N., Haghani, S., Zeinali, H., & Roghani, M. (2017). The anti-aging protein klotho alleviates injury of nigrostriatal dopaminergic pathway in 6-hydroxydopamine rat model of Parkinson's disease: Involvement of PKA/CaMKII/CREB signaling. *Experimental Gerontology*, *100*, 70–76. <https://doi.org/10.1016/j.exger.2017.10.023>
- Bian, A., Neyra, J. A., Zhan, M., & Hu, M. C. (2015). Klotho, stem cells, and aging. *Clinical Interventions in Aging*, *10*, 1233–1243. <https://doi.org/10.2147/CIA.S84978>
- Cai, Z., Liu, N., Wang, C., Qin, B., Zhou, Y., Xiao, M., ... Zhao, B. (2016). Role of RAGE in Alzheimer's disease. *Cellular and Molecular Neurobiology*, *36*(4), 483–495. <https://doi.org/10.1007/s10571-015-0233-3>
- Chiu, C., Miller, M. C., Caralopoulos, I. N., Worden, M. S., Brinker, T., Gordon, Z. N., ... Silverberg, G. D. (2012). Temporal course of cerebrospinal fluid dynamics and amyloid accumulation in the aging rat brain from three to thirty months. *Fluids and Barriers of the CNS*, *9*(1), 3. <https://doi.org/10.1186/2045-8118-9-3>
- Chiu, C., Miller, M. C., Monahan, R., Osgood, D. P., Stopa, E. G., & Silverberg, G. D. (2015). P-glycoprotein expression and amyloid accumulation in human aging and Alzheimer's disease: Preliminary observations. *Neurobiology of Aging*, *36*(9), 2475–2482.
- Dinner, S., Borkowski, J., Stump-Guthier, C., Ishikawa, H., Tenenbaum, T., Schrotten, H., & Schwerk, C. (2016). A choroid plexus epithelial cell-based model of the human blood-cerebrospinal fluid barrier to study bacterial infection from the basolateral side. *Journal of Visualized Experiments*, *111*, 54061. <https://doi.org/10.3791/54061>
- Dubal, D. B., Yokoyama, J. S., Zhu, L., Broestl, L., Worden, K., Wang, D., ... Mucke, L. (2014). Life extension factor klotho enhances cognition. *Cell Reports*, *7*(4), 1065–1076. <https://doi.org/10.1016/j.celrep.2014.03.076>
- Dubal, D. B., Zhu, L., Sanchez, P. E., Worden, K., Broestl, L., Johnson, E., ... Mucke, L. (2015). Life extension factor klotho prevents mortality and enhances cognition in hAPP transgenic mice. *Journal of Neuroscience*, *35*(6), 2358–2371. <https://doi.org/10.1523/JNEUROSCI.5791-12.2015>
- Elali, A., & Rivest, S. (2013). The role of ABCB1 and ABCA1 in beta-amyloid clearance at the neurovascular unit in Alzheimer's disease. *Frontiers in Physiology*, *4*, 45. <https://doi.org/10.3389/fphys.2013.00045>
- Erickson, M. A., & Banks, W. A. (2013). Blood-brain barrier dysfunction as a cause and consequence of Alzheimer's disease. *Journal of Cerebral Blood Flow and Metabolism*, *33*(10), 1500–1513. <https://doi.org/10.1038/jcbfm.2013.135>
- Frautschy, S. A., Yang, F., Irrizarry, M., Hyman, B., Saido, T. C., Hsiao, K., & Cole, G. M. (1998). Microglial response to amyloid plaques in APPsw transgenic mice. *American Journal of Pathology*, *152*(1), 307–317.



- Greenberg, S. M., Bacsikai, B. J., Hernandez-Guillamon, M., Pruzin, J., Sperling, R., & van Veluw, S. J. (2020). Cerebral amyloid angiopathy and Alzheimer disease – One peptide, two pathways. *Nature Reviews Neurology*, 16(1), 30–42. <https://doi.org/10.1038/s41582-019-0281-2>
- Guo, Y. X., He, L. Y., Zhang, M., Wang, F., Liu, F., & Peng, W. X. (2016). 1,25-Dihydroxyvitamin D3 regulates expression of LRP1 and RAGE in vitro and in vivo, enhancing A β 1-40 brain-to-blood efflux and peripheral uptake transport. *Neuroscience*, 322, 28–38. <https://doi.org/10.1016/j.neuroscience.2016.01.041>
- Hardy, J. A., & Higgins, G. A. (1992). Alzheimer's disease: The amyloid cascade hypothesis. *Science*, 256(5054), 184–185. <https://doi.org/10.1126/science.1566067>
- Heneka, M. T., Kummer, M. P., Stutz, A., Delekate, A., Schwartz, S., Vieira-Saecker, A., ... Golenbock, D. T. (2013). NLRP3 is activated in Alzheimer's disease and contributes to pathology in APP/PS1 mice. *Nature*, 493(7434), 674–678. <https://doi.org/10.1038/nature11729>
- Ising, C., Venegas, C., Zhang, S., Scheiblich, H., Schmidt, S. V., Vieira-Saecker, A., ... Heneka, M. T. (2019). NLRP3 inflammasome activation drives tau pathology. *Nature*, 575(7784), 669–673. <https://doi.org/10.1038/s41586-019-1769-z>
- Kuang, X., Zhou, H. J., Thorne, A. H., Chen, X. N., Li, L. J., & Du, J. R. (2017). Neuroprotective effect of ligustilide through induction of α -secretase processing of both APP and Klotho in a mouse model of Alzheimer's disease. *Frontiers in Aging Neuroscience*, 9, 353. <https://doi.org/10.3389/fnagi.2017.00353>
- Kuplennik, N., Lang, K., Steinfeld, R., & Sosnik, A. (2019). Folate receptor α -modified nanoparticles for targeting of the central nervous system. *ACS Applied Materials & Interfaces*, 11(43), 39633–39647. <https://doi.org/10.1021/acsami.9b14659>
- Kuro-o, M., Matsumura, Y., Aizawa, H., Kawaguchi, H., Suga, T., Utsugi, T., ... Nabeshima, Y.-I. (1997). Mutation of the mouse klotho gene leads to a syndrome resembling ageing. *Nature*, 390(6655), 45–51. <https://doi.org/10.1038/36285>
- Kurosu, H., Yamamoto, M., Clark, J. D., Pastor, J. V., Nandi, A., Gurnani, P., ... Kuro-o, M. (2005). Suppression of aging in mice by the hormone Klotho. *Science*, 309(5742), 1829–1833. <https://doi.org/10.1126/science.1112766>
- Li, D., Jing, D., Liu, Z., Chen, Y., Huang, F., & Behnisch, T. (2019). Enhanced expression of secreted α -klotho in the hippocampus alters nesting behavior and memory formation in mice. *Frontiers in Cellular Neuroscience*, 13, 133. <https://doi.org/10.3389/fncel.2019.00133>
- Lim, K., Groen, A., Molostvov, G., Lu, T., Lilley, K. S., Snead, D., ... Zehnder, D. (2015). α -Klotho expression in human tissues. *Journal of Clinical Endocrinology and Metabolism*, 100(10), E1308–E1318. <https://doi.org/10.1210/jc.2015-1800>
- Martiskainen, H., Haapasalo, A., Kurkinen, K. M., Pihlajamäki, J., Soininen, H., & Hiltunen, M. (2013). Targeting ApoE4/ApoE receptor LRP1 in Alzheimer's disease. *Expert Opinion on Therapeutic Targets*, 17(7), 781–794. <https://doi.org/10.1517/14728222.2013.789862>
- Massó, A., Sánchez, A., Gimenez-Llort, L., Lizcano, J. M., Cañete, M., García, B., ... Chillón, M. (2015). Secreted and transmembrane α -klotho isoforms have different spatio-temporal profiles in the brain during aging and Alzheimer's disease progression. *PLoS One*, 10(11), e0143623. <https://doi.org/10.1371/journal.pone.0143623>
- Masters, C. L., Bateman, R., Blennow, K., Rowe, C. C., Sperling, R. A., & Cummings, J. L. (2015). Alzheimer's disease. *Nature Reviews Disease Primers*, 1, 15056. <https://doi.org/10.1038/nrdp.2015.56>
- Nalivaeva, N. N., & Turner, A. J. (2019). Targeting amyloid clearance in Alzheimer's disease as a therapeutic strategy. *British Journal of Pharmacology*, 176(18), 3447–3463. <https://doi.org/10.1111/bph.14593>
- Ng, R. C.-L., Jian, M., Ma, O. K.-F., Bunting, M., Kwan, J. S.-C., Zhou, G.-J., ... Chan K.-H. (2020). Chronic oral administration of adipoRon reverses cognitive impairments and ameliorates neuropathology in an Alzheimer's disease mouse model. *Molecular Psychiatry*. <http://dx.doi.org/10.1038/s41380-020-0701-0>
- Saresella, M., La Rosa, F., Piancone, F., Zoppis, M., Marventano, I., Calabrese, E., ... Clerici, M. (2016). The NLRP3 and NLRP1 inflammasomes are activated in Alzheimer's disease. *Molecular Neurodegeneration*, 11, 23. <https://doi.org/10.1186/s13024-016-0088-1>
- Scazzone, C., Agnello, L., Lo Sasso, B., Ragonese, P., Bivona, G., Realmuto, S., ... Ciaccio, M. (2019). Klotho and vitamin D in multiple sclerosis: An Italian study. *Archives of Medical Science*, 16(4), 842–847. <https://doi.org/10.5114/aoms.2019.86969>
- Selkoe, D. J., & Hardy, J. (2016). The amyloid hypothesis of Alzheimer's disease at 25 years. *EMBO Molecular Medicine*, 8(6), 595–608. <https://doi.org/10.15252/emmm.201606210>
- Semba, R. D., Moghekar, A. R., Hu, J., Sun, K., Turner, R., Ferrucci, L., & O'Brien, R. (2014). Klotho in the cerebrospinal fluid of adults with and without Alzheimer's disease. *Neuroscience Letters*, 558, 37–40. <https://doi.org/10.1016/j.neulet.2013.10.058>
- Serot, J.-M., Peltier, J., Fichten, A., Ledeme, N., Bourgeois, A.-M., Jouanny, P., ... Mazière, J.-C. (2011). Reduced BCF turnover and decreased ventricular A β 42 levels are related. *BMC Neuroscience*, 12, 42. <https://doi.org/10.1186/1471-2202-12-42>
- Sheedy, F. J., Grebe, A., Rayner, K. J., Kalantari, P., Ramkhalawon, B., Carpenter, S. B., ... Moore, K. J. (2013). CD36 coordinates NLRP3 inflammasome activation by facilitating intracellular nucleation of soluble ligands into particulate ligands in sterile inflammation. *Nature Immunology*, 14(8), 812–820. <https://doi.org/10.1038/ni.2639>
- Silverberg, G. D., Miller, M. C., Messier, A. A., Majmudar, S., Machan, J. T., Donahue, J. E., ... Johanson, C. E. (2010). Amyloid deposition and influx transporter expression at the blood-brain barrier increase in normal aging. *Journal of Neuropathology and Experimental Neurology*, 69(1), 98–108. <https://doi.org/10.1097/NEN.0b013e3181c8ad2f>
- Takechi, R., Galloway, S., Pallebage-Gamarallage, M. M., Wellington, C. L., Johnsen, R. D., Dhaliwal, S. S., & Mamo, J. C. (2010). Differential effects of dietary fatty acids on the cerebral distribution of plasma-derived apo B lipoproteins with amyloid-beta. *British Journal of Nutrition*, 103(5), 652–662. <https://doi.org/10.1017/S000711450992194>
- Wang, J., Gu, B. J., Masters, C. L., & Wang, Y. J. (2017). A systemic view of Alzheimer disease – Insights from amyloid- β metabolism beyond the brain. *Nature Reviews Neurology*, 13(10), 612–623. <https://doi.org/10.1038/nrneuro.2017.111>
- Xin, S. H., Tan, L., Cao, X., Yu, J. T., & Tan, L. (2018). Clearance of amyloid beta and tau in Alzheimer's disease: From mechanisms to therapy. *Neurotoxicity Research*, 34(3), 733–748. <https://doi.org/10.1007/s12640-018-9895-1>
- Xu, Y., & Sun, Z. (2015). Molecular basis of Klotho: From gene to function in aging. *Endocrine Reviews*, 36(2), 174–193. <https://doi.org/10.1210/er.2013-1079>
- Yin, J., Zhao, F., Chojnacki, J. E., Fulp, J., Klein, W. L., Zhang, S., & Zhu, X. (2018). NLRP3 inflammasome inhibitor ameliorates amyloid pathology in a mouse model of Alzheimer's disease. *Molecular Neurobiology*, 55(3), 1977–1987. <https://doi.org/10.1007/s12035-017-0467-9>
- Zeldich, E., Chen, C.-D., Boden, E., Howat, B., Nasse, J. S., Zeldich, D., ... Abraham, C. R. (2019). Klotho is neuroprotective in the superoxide dismutase (SOD1^{G93A}) mouse model of ALS. *Journal of Molecular Neuroscience*, 69(2), 264–285. <https://doi.org/10.1007/s12035-019-01356-2>
- Zeng, C. Y., Yang, T. T., Zhou, H. J., Zhao, Y., Kuang, X., Duan, W., & Du, J. R. (2019). Lentiviral vector-mediated overexpression of Klotho in the brain improves Alzheimer's disease-like pathology and cognitive deficits in mice. *Neurobiology of Aging*, 78, 18–28. <https://doi.org/10.1016/j.neurobiolaging.2019.02.003>



- Zhang, S., Zhi, Y., Li, F., Huang, S., Gao, H., Han, Z., ... Lei, P. (2018). Transplantation of in vitro cultured endothelial progenitor cells repairs the blood-brain barrier and improves cognitive function of APP/PS1 transgenic AD mice. *Journal of the Neurological Sciences*, 387, 6–15. <https://doi.org/10.1016/j.jns.2018.01.019>
- Zheng, W., & Zhao, Q. (2002). The blood-CSF barrier in culture. Development of a primary culture and transepithelial transport model from choroidal epithelial cells. *Methods in Molecular Biology*, 188, 99–114. <https://doi.org/10.1385/1-59259-185-X:99>
- Zhu, D., Su, Y., Fu, B., & Xu, H. (2018). Magnesium reduces blood-brain barrier permeability and regulates amyloid- β transcytosis. *Molecular Neurobiology*, 55(9), 7118–7131. <https://doi.org/10.1007/s12035-018-0896-0>
- Zhu, L., Stein, L. R., Kim, D., Ho, K., Yu, G.-Q., Zhan, L., ... Mucke, L. (2018). Klotho controls the brain-immune system interface in the choroid plexus. *Proceedings of the National Academy of Sciences of*

the United States of America, 115(48), E11388–E11396. <https://doi.org/10.1073/pnas.1808609115>

SUPPORTING INFORMATION

Additional supporting information may be found online in the Supporting Information section.

How to cite this article: Zhao Y, Zeng CY, Li XH, Yang TT, Kuang X, Du JR. Klotho overexpression improves amyloid- β clearance and cognition in the APP/PS1 mouse model of Alzheimer's disease. *Aging Cell*. 2020;19:e13239. <https://doi.org/10.1111/ace1.13239>